Theoretical Study on the Mechanisms of Catalytic Hydration of Diiodine Trioxide in Marine Regions

Yan Liang[1], Xiuhui Zhang[1,*], and Wenguo Xu[1,*]

[1]School of Chemistry and Chemical Engineering, Beijing Institute of Technology, Beijing 100081, China.

Abstract. Diiodine trioxide (I_2O_3) is one of the most common iodine oxides in the marine boundary layer (MBL). Both theoretical and experimental studies have confirmed that they can be quickly formed and are relatively stable under dry conditions. However, there is no report on the field observation of I_2O_3, which means that I_2O_3 is likely to be lost in the actual marine atmosphere. But the specific loss pathways and mechanisms are still unclear. Considering that the humidity in the marine regions is generally high and the loss of I_2O_3 will be affected by some substances in the marine atmosphere, water (H_2O, **W**) and iodic acid (HIO_3, **IA**) were selected as a catalyst to investigate the catalytic hydration mechanisms of I_2O_3 at DLPNO-CCSD(T)//ωB97X-D/aug-cc-pVTZ + aug-cc-pVTZ -PP (for iodine) level of theory. The results show that hydration of I_2O_3 presents a high energy barrier, but **IA** can reduce it to 3.76 kcal/mol. Therefore, in the marine atmosphere, I_2O_3 can be hydrolyzed under the catalysis of **IA**, and cannot directly participate in the new particle formation process.

1 Introduction

Atmospheric aerosols have great impacts on human health and the atmospheric environment ([1]). Ultrafine aerosols (particle matter with a size of less than 2.5μm) are key components of local and regional air pollution. There is increasing evidence that exposure to ultrafine aerosols can cause some acute and chronic diseases ([2]). In addition, aerosols can also affect the cloud formation process by increasing the total amount of cloud condensation nuclei (CNN), which in turn has an important impact on the climate ([3]). Marine covers 71% of the total surface of the earth, thus, marine aerosols have a non-negligible position in the global aerosol system. In recent years, the outbreaks of ultrafine particles have been frequently observed in marine areas ([4-7]). Researchers have confirmed that the formation of new particles in the marine regions is linked to the iodine-containing substances in the marine atmosphere.

Diiodine trioxide (I_2O_3) is a common iodine oxide in the marine boundary layer (MBL) ([8]). A laboratory study has shown that the polymerization between IO and OIO radicals will generate I_2O_3 ([9]). Lifetime calculation showed that the time for I_2O_3 to resist pyrolysis is 1.67×10^{11} s ([10]), indicating that I_2O_3 can therefore remain in the marine atmosphere for a certain period. However, so far, there is no report on the field observation of I_2O_3, which means that I_2O_3 is likely to be lost due to certain reactions in the actual marine atmosphere. But the specific loss pathways and mechanisms are still unclear, which greatly affects people's understanding of the biogeochemical cycle of iodine. Considering that the humidity in the marine regions is generally high and the loss of I_2O_3 will be affected by some substances in the marine atmosphere, it is speculated that I_2O_3 may be hydrolyzed in the gas phase. Thus, common substances in the marine atmosphere, water (H_2O, **W**) and iodic acid (HIO_3, **IA**), were selected as a catalyst to investigate the catalytic hydration reaction mechanisms of I_2O_3.

In the present paper, the hydrations of I_2O_3 without catalyst and catalyzed by **W** as well as **IA** were studied at DLPNO-CCSD(T)//ωB97X-D/aug-cc-pVTZ + aug-cc-pVTZ-PP level of theory to explore whether hydration is one of the loss pathways of I_2O_3.

2 Methods

The method of quantum chemistry calculation is used to study the hydration reactions of I_2O_3 when common substances **W** and **IA** in the marine atmosphere act as catalysts. The configurations of the stationary points and transition states are optimized by using the Gaussian-09 ([11]) software package at 298 K and 1 atm. All calculations are performed at DLPNO-CCSD(T)//ωB97X-D/aug-cc-pVTZ + aug-cc-pVTZ-PP level of theory ([12]). The aug-cc-pVTZ-PP basis set with effective core potential ECP28MDF ([13,14]) is used for the iodine atom and the conventional aug-cc-pVTZ ([15]) basis set for the other atoms. And intrinsic reaction coordinate (IRC) calculations were performed to ensure the translation states were correctly connected to the corresponding reactants and products. And the Gibbs free energies (G) of compounds were calculated as:

$$G = E_{SPE} + G_{thermal} \quad (1)$$

* Corresponding author: zhangxiuhui@bit.edu.cn, xuwg60@bit.edu.cn

where E_{SPE} is the single-point energy calculated by the DLPNO-CCSD(T) method, and $G_{thermal}$ is the thermal corrections to Gibbs free energy calculated by the ωB97X-D method.

In order to predict the reaction sites of I_2O_3 hydration, Multiwfn 3.6 ([16]) and Visual Molecular Dynamics (VMD) ([17]) software were also used to analyze the electrostatic potential (ESP) ([18]) on the molecular surface and draw ESP-mapped of molecular van der Waals (vdW) surfaces of reactants.

3 Results and discussion

3.1. The hydration of I_2O_3 without catalysts

In order to explore the reaction sites of I_2O_3 hydration, the electrostatic potential (ESP) on the surfaces of I_2O_3 and **W** molecules was first analyzed. As shown in **Fig. 1**, the two hydrogen atoms of **W** have a relatively positive electrostatic potential (red area), and the two oxygen atoms of I_2O_3 have a relatively negative electrostatic potential (blue area). Therefore, the complex I_2O_3-H_2O (**I_2O_3-W**) can be formed through electrostatic attraction between **W** and I_2O_3.

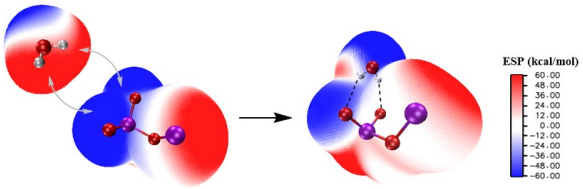

Fig. 1. The ESP-mapped molecular vdW surfaces of reactants I_2O_3 and **W** as well as the pre-reaction complex **I_2O_3-W**. The purple, red, and grey spheres represent **I**, **O**, and **H** atoms, respectively. The black and grey dashed line refers to the hydrogen bond between I_2O_3 and **W**, respectively.

Subsequently, the I_2O_3 hydration reaction was calculated at the DLPNO-CCSD(T)//ωB97X-D/ aug-cc-pVTZ (H, C, N, O, S) + aug-cc-pVTZ-PP (for iodine) level of theory. Take the sum of Gibbs free energies (G) of the reactants as the zero point of the potential energy surface. **Fig. 2** (a) is the potential energy surface of the I_2O_3 hydration reaction, and **Fig. 2** (b) is the corresponding energy profile. The hydration of I_2O_3 starts with the collision between I_2O_3 and **W** molecules to form the pre-reaction complex **I_2O_3-W** with a relative Gibbs free energy of 4.31 kcal/mol. Then, **I_2O_3-W** overcomes a relatively high Gibbs free energy barrier of 32.60 kcal/mol to generate the product HIO_3-HOI (**IA-HA**). The energy barrier of the reaction is as high as 32.60 kcal/mol, and it is an endothermic reaction, indicating that without the participation of catalysts, the hydration reaction of I_2O_3 is difficult to occur in the actual marine atmosphere.

On this basis, the mechanism of I_2O_3 hydration was further analyzed. As shown in **Fig. 2** (a), a proton of **W** transfers to the **O** atom of I_2O_3 while the **OH** moiety binds to the **I** atom of I_2O_3 to form the product. Therefore, the nature of the I_2O_3 hydration is the transfer of a hydrogen proton.

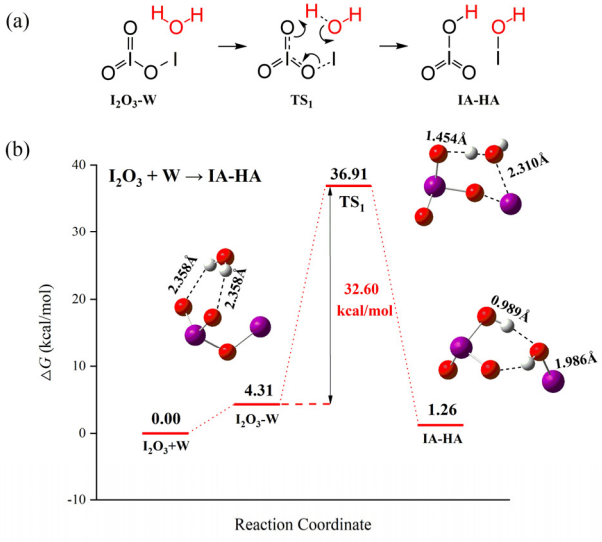

Fig. 2. (a) Reaction mechanism for the gas-phase hydration of I_2O_3 with no catalyst. (b) Potential energy profiles (kcal/mol) for gas-phase hydration of I_2O_3 with no catalyst calculated at DLPNO-CCSD(T)//ωB97X-D/aug-cc-pVTZ + aug-cc-pVTZ-PP (for iodine) level of theory at 298 K and 1 atm. The purple, red, and white spheres represent I, O, and H atoms, respectively.

3.2 The hydration of I_2O_3 catalyzed by W

The marine atmosphere is very humid, so the concentration of **W** is generally high. **W** can act as a proton acceptor and donor at the same time, thereby accelerating the transfer of protons between molecules, so **W** may be used as a catalyst. In this section, the hydration reaction of I_2O_3 when **W** acts as a catalyst was studied. **Fig. 3** (a) shows the I_2O_3 hydration mechanism catalyzed by **W**, and **Fig. 3** (b) shows the potential energy surface of the corresponding reaction.

As shown in **Fig. 3** (b), the catalytic hydration of I_2O_3 has two pathways: I_2O_3 first collides with **W** to form **I_2O_3-W** and two **W** molecules collide first to form **W-W** dimer. The pathway that first forms the **W-W** dimer requires the lowest energy and is the main pathway. Then, **W-W** collides with I_2O_3 to form the pre-reaction complex **I_2O_3-W-W**, and **I_2O_3-W-W** overcomes a relatively Gibbs free energy barrier of 16.91 kcal/mol to generate the product HIO_3-HOI-H_2O (**IA-HA-W**). The catalytic reaction is endothermic and there is a certain energy barrier. Therefore, when **W** acts as a catalyst, the hydration reaction of I_2O_3 is unfavorable in both kinetics and thermodynamics.

It is worth noting that, compared with the reaction of I_2O_3 without a catalyst, **W** as a catalyst effectively reduces the energy barrier from 32.60 kcal/mol to 16.91 kcal/mol. This is because, with the participation of the catalyst **W**, the transition state changes from the original six-membered ring structure to an eight-membered ring structure, and the ring strain of the transition state is therefore reduced, so the energy barrier becomes lower. When **W** acts as a catalyst, it assists the transfer of protons between molecules by accepting and donating protons simultaneously. In summary, **W** as a catalyst

assists the transfer of protons between molecules, thereby lowering the energy barrier.

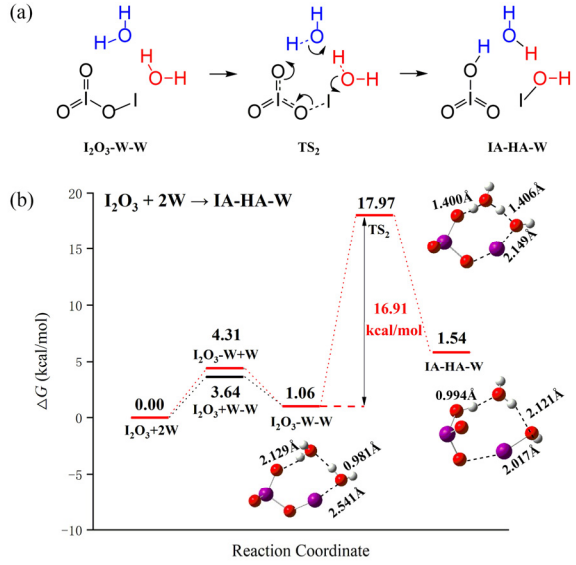

Fig. 3. (a) Reaction mechanism for the gas-phase hydration of I_2O_3 catalyzed by **W**. (b) Potential energy profiles (kcal/mol) for gas-phase hydration of I_2O_3 catalyzed by **W** calculated at DLPNO-CCSD(T)//ωB97X-D/aug-cc-pVTZ + aug-cc-pVTZ-PP (for iodine) level of theory at 298 K and 1 atm. The purple, red, and white spheres represent I, O, and H atoms, respectively.

3.3 The hydration of I_2O_3 catalyzed by IA

As discussed above, the nature of the I_2O_3 hydration is the transfer of protons between I_2O_3 and **W**. As one of the hydration products of I_2O_3, **IA** is very common in marine atmosphere and has a relatively high concentration ([21]), and it can act as both an acceptor and a donor of protons. Thus, it is necessary to study whether **IA** can catalyze the hydration of I_2O_3 by assisting the transfer of protons. **Fig. 3** (a) shows the I_2O_3 hydration mechanism catalyzed by **IA**, and **Fig. 3** (b) shows the potential energy surface of the corresponding reaction.

There are three different bi-molecular collision modes between I_2O_3, **IA**, and **W** (**I_2O_3-W**, **I_2O_3-IA**, and **IA-W**) so there are three pathways for the catalytic reaction. The formation of **I_2O_3-W** and **I_2O_3-IA** is endothermic, so these two pathways are not likely to occur in the actual marine atmosphere. The pathway that first forms the **IA-W** is exothermic, thus it is the main pathway. And **IA-W** collides with I_2O_3 to form pre-reaction complex **I_2O_3-IA-W**, which then forms **$(IA)_2$-HA** by a stepwise mechanism. This reaction has a very low energy barrier (3.76 kcal/mol) and is exothermic, so it is kinetically and thermodynamically favorable. In addition, the energy released by the formation of the reaction complex **I_2O_3-IA-W** is higher than the energy barrier, so the reaction can occur spontaneously in the common marine atmosphere. It should be noted that the Gibbs free energy of the Intermediate (**Int**) is slightly higher than that of Transition State 2 (**TS_2**) because of the calculation error, which is caused by the approximate electron density used in the DFT calculations, and it always occurs in systems involving proton transfer ([18,19]).

As shown in **Fig. 4** (a), the participation of the catalyst **IA** changed the transition state into a ten-membered ring structure, which further reduces the ring strain of the transition states and makes the reaction energy barrier lower (3.76 kcal/mol). The specific catalytic mechanism is that **IA** first gives a proton to I_2O_3, thus, forming the intermediate (**Int**) HIO_3-IH_2O^+-IO_3^-, and then IO_3^- accepts the proton from **W** to form the product **$(IA)_2$-HA**. The mechanisms of **IA** catalytic and **W** catalytic are similar, the **IA** and **W** both assist the transfer of protons between I_2O_3 and **W** by accepting and donating protons. The difference is that when **IA** acts as a catalyst, the transfer of protons is step by step, but the transfer of protons is simultaneous when **W** acts as a catalyst. Compared with **W**, **IA** is a stronger proton donor and is easier to give protons, so the energy barrier is lower than when **W** catalyzing.

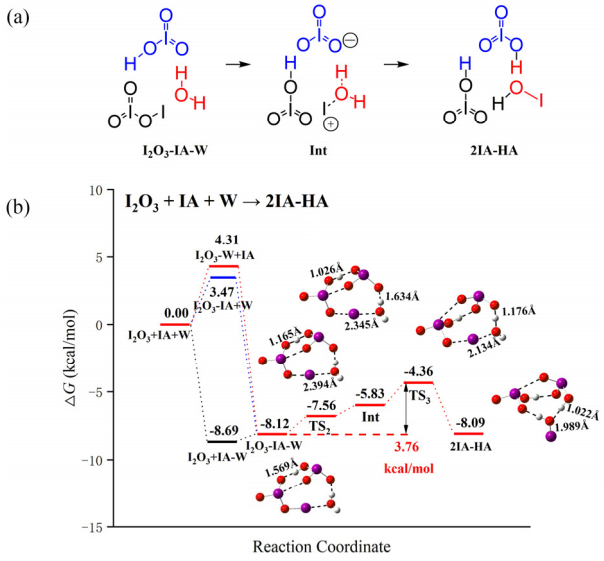

Fig. 4. (a) Reaction mechanism for the gas-phase hydration of I_2O_3 catalyzed by **IA**. (b) Potential energy profiles (kcal/mol) for gas-phase hydration of I_2O_3 catalyzed by **IA** calculated at DLPNO-CCSD(T)//ωB97X-D/aug-cc-pVTZ + aug-cc-pVTZ-PP (for iodine) level of theory at 298 K and 1 atm. The purple, red, and white spheres represent I, O, and H atoms, respectively.

4 Conclusions

The gas-phase hydrations of I_2O_3 with no catalyst and with common atmospheric substances **W** and **IA** as catalysts were calculated at DLPNO-CCSD(T)//ωB97X-D/aug-cc-pVTZ + aug-cc-pVTZ-PP (for iodine) level of theory. The results showed that under the catalysis of **W** and **IA**, the energy barrier is reduced. Especially under the catalysis of **IA**, the energy barrier can be reduced to 3.76 kcal/mol, and the catalytic reaction spontaneously occurred. **IA** is both one of the products of the I_2O_3 hydration reaction and a catalyst, so the reaction can be autocatalyzed. The concentration of **IA** gradually

increases as the reaction proceeds, so the role of **IA** in the I_2O_3 hydration gradually increases. Thus, I_2O_3 is unstable and short-lived, and much likely to undergo hydration to generate **IA** in the marine regions, which is one of the loss pathways of I_2O_3. I_2O_3 cannot directly participate in the formation of new particles in the marine atmosphere, but the products **IA** may be involved in the nucleation process, therefore catalytic hydration reaction may trigger the formation of new particles.

This research can provide a comprehensive understanding of the biogeochemical cycle of iodine and provide theoretical guidance for the formation of new particles in marine and coastal regions.

References

1. Murphy D.M. Ravishankara A.R. Trends and patterns in the contributions to cumulative radiative forcing from different regions of the world. Proc Natl Acad Sci U S A. 115,52 (2018)
2. Gong J.C. Zhu T. Kipen H. et al. Comparisons of Ultrafine and Fine Particles in Their Associations with Biomarkers Reflecting Physiological Pathways. Environ Sci Technol. 48, 9 (2014)
3. Glasow R. Seaweed, Iodine, New Particles and Atmospheric Chemistry - The Current State of Play. Environ Chem. 2, 4 (2005)
4. Dall´Osto M. Simo R. Harrison R.M. et al. Abiotic and biotic sources influencing spring new particle formation in North East Greenland. Atmos Environ. 190 (2018).
5. McFiggans G. Coe H. Burgess R. et al. Direct evidence for coastal iodine particles from Laminaria macroalgae - linkage to emissions of molecular iodine. Atmos Chem Phys. 4 (2004)
6. Jimenez J.L Bahreini R. Cocker III D.R. et al. New particle formation from photooxidation of diiodomethane (CH_2I_2). J Geophys Res. 108, D10 (2003)
7. Saiz-Lopez A. Plane J.M.C. Novel iodine chemistry in the marine boundary layer. Geophys Res Lett. 31, 4 (2004)
8. Saiz-Lopez A. Plane J.M. Baker A.R. et al. Atmospheric Chemistry of Iodine. Chem Rev. 112, 3 (2012)
9. Galvez O. Gomez Martin J.C. Gomez P.C. et al. A theoretical study on the formation of iodine oxide aggregates and monohydrates. Phys Chem Chem Phys. 15, 3 (2013)
10. Gomez Martin J.C. Galvez O. Baeza-Romero M.T. et al. On the mechanism of iodine oxide particle formation. Phys Chem Chem Phys. 15, 37 (2013)
11. Frisch M.J. Trucks G.W. Schlegel H.B. et al. Gaussian 09, Revision A.1, Gaussian, Inc. Wallingford, CT. (2009)
12. Peterson K.A. Systematically Convergent Basis Sets with Relativistic Pseudopotentials. I. Correlation Consistent Basis Sets for the Post-D Group 13–15 Elements. J Chem Phys. 119, 21 (2003)
13. Feller D. The role of databases in support of computational chemistry calculations. J Comput Chem. 17, 13 (1996)
14. Schuchardt K.L. Didier B.T. Elsethagen T. et al. Basis set exchange: a community database for computational sciences. J Chem Inf Model. 47, 3 (2007)
15. Peterson K.A. Systematically Convergent Basis Sets with Relativistic Pseudopotentials. I. Correlation Consistent Basis Sets for the Post-D Group 13–15 Elements. J Chem Phys. 119, 21 (2003)
16. Lu T. Chen F. Multiwfn: a multifunctional wavefunction analyzer. J Comput Chem, 33, 5 (2012)
17. Humphrey W. Dalke A. Schulten K. VMD: visual molecular dynamics. J Mol Graph. 14, 1 (1996)
18. Mohan N. Suresh C.H. A molecular electrostatic potential analysis of hydrogen, halogen, and dihydrogen bonds. J Phys Chem A. 118, 9 (2014)
19. You Z.S.; Guo C. Pan Y.J. An experimental and theoretical study on fragmentation of protonated N-(2-pyridinylmethyl) indole in electrospray ionization mass spectrometry. Rapid Commun Mass Spectrom. 26, (2012)
20. Kim M.C. Sim E. Burke K. Understanding and reducing errors in density functional calculations. Phys Rev Lett. 111,7 (2013)
21. Sipila M. Sarnela N. Jokinen T. et al. Molecular-scale evidence of aerosol particle formation via sequential addition of HIO_3. Nature. 537, 7621 (2016)